



ELSEVIER

Journal of Chromatography A, 824 (1998) 159–167

JOURNAL OF  
CHROMATOGRAPHY A

# High-performance liquid chromatography with real-time Fourier-transform infrared detection for the determination of carbohydrates, alcohols and organic acids in wines

R. Vonach, B. Lendl\*, R. Kellner<sup>†</sup>

*Institute for Analytical Chemistry, Vienna University of Technology, A-1060 Vienna, Austria*

Received 14 October 1997; received in revised form 12 May 1998; accepted 7 July 1998

## Abstract

The coupling of high-performance liquid chromatography (HPLC) with Fourier-transform infrared spectroscopy (FTIR) is presented as a new and versatile tool for the direct determination of the main components of wine, which are glucose, fructose, glycerol, ethanol, acetic, citric, lactic, malic, succinic and tartaric acid. An ion-exchange resin based column (counterion:  $H^+$ ) was employed as the stationary phase and 0.005 M sulfuric acid as the mobile phase. FTIR detection in the spectral region from 1600 to 900  $cm^{-1}$  was performed in a 25- $\mu m$  flow cell without elimination of the solvent. Characteristic FTIR spectra were obtained subsequent to the injection and separation of 2 mg/ml of each component. The average standard deviation of the investigated compounds was found to be 66  $\mu g/ml$  in standard solutions containing 1–10 mg/ml of the analyte. The method was furthermore applied to real wine samples taken from a round robin test. An average deviation of 0.16 mg/ml from the external reference data was obtained. © 1998 Elsevier Science B.V. All rights reserved.

**Keywords:** Detection, LC; Fourier-transform infrared spectrometry; Wine; Carbohydrates; Alcohols; Organic acids

## 1. Introduction

The development of a molecular specific detection system for high-performance liquid chromatography (HPLC) is an ongoing research field in analytical chemistry. Since most compounds absorb in the infrared region, Fourier-transform infrared spectroscopy (FTIR) can provide qualitative information about compounds. This is of particular interest for analytes such as carbohydrates or alcohols that are

not or only poorly detectable by standard UV spectrometry.

The opacity of the mobile phase is the most important factor for limiting the field of application for FTIR detection in liquid chromatography. Especially in reversed phase chromatography and other applications operating with aqueous eluents, the successful application of FTIR detection is hampered by the large water bands in the mid IR region [1–4]. To overcome solvent interference, much work has already been done focusing on various solvent elimination approaches. In the case of aqueous mobile phases as they are applied in reversed-phase (RP) and in the described application of ion-exchange chromatography, the low volatility of water

\*Corresponding author. Fax: +43-1-5867813; E-mail: blendl@fbch.tuwien.ac.at

<sup>†</sup>Professor Robert Kellner deceased 8 October, 1997

requires sophisticated solvent elimination approaches. The use of microbore columns is often necessary to reduce the effluent flow. Among various methods, the introduction of nitrogen into the carrier flow [5], the use of a concentric flow nebulizer [6–8], and ultrasonic [9] or electrospray [10] nebulization have been applied for the elimination of aqueous solvents. Some authors have also employed a particle beam interface [11–14] (originally designed for HPLC–MS) or a thermospray interface [15–17].

Other solvent elimination approaches are based on postcolumn on-line extraction to achieve compatibility between FTIR detection and RP chromatography. After extraction of the analytes with chlorinated solvents ( $\text{CH}_2\text{Cl}_2$ ,  $\text{CHCl}_3$ ,  $\text{CCl}_4$ ), various interfaces can be applied, such as regular flow cells [18,19], the deposition of the extracts on KCl powder with subsequent diffuse reflectance infrared detection (DRIFT) [20] or, more recently, deposition on a zinc selenide window by a spray jet assembly, followed by analysis of the residues with an FTIR microscope [21].

In contrast to these methods, this work is dealing with a flow cell FTIR interface without solvent elimination. In this case, two IR-transparent windows are separated by a lead or PTFE spacer providing an optical path length generally between 10 to 200  $\mu\text{m}$ , dependent on the IR-transparency of the mobile phase. If short path lengths of 20  $\mu\text{m}$  or less are required, the use of internal reflectance flow cells (Circle<sup>®</sup> cell) has also been reported. Cylindrical ZnSe rods serve as an attenuated total reflectance (ATR) element to perform internal reflection measurements [22–24]. One approach for diminishing the spectral overlap between solvent and analyte is the utilization of deuterated mobile phases. Of course, they are only cost-effectively applied in microbore HPLC [25,26]. RP- and size-exclusion chromatography (SEC) separations in the low microgram range have been reported so far using  $\text{C}^2\text{H}_3\text{CN}-^2\text{H}_2\text{O}$  and  $^2\text{H}_2\text{O}$  mobile phases [27].

Among the very few applications dealing with aqueous phase HPLC and flow cell FTIR interfaces, one paper describes the separation of a mixture of acetophenone, ethylbenzoate and nitrobenzene (1–2%) followed by IR detection using a Circle<sup>®</sup> cell [22]. In another contribution, structural information

on metallocene–amino acid adducts has been gained after the separation of 0.7 mg of the analytes [28]. The separation of caffeine and theophylline, again using the Circle<sup>®</sup> cell, has also been reported, with detection limits of the order of 0.2% (0.1 mg) [24]. In a previous work by our group [29], the determination of sucrose, glucose and fructose in fruit juices was successfully performed using an IR flow cell for transmission measurements.

In this work, the applicability of an advanced flow cell HPLC–FTIR setup was studied with the aim of determining the carbohydrates, alcohols and organic acids present in complex matrices such as wines. The principal capability of gaining qualitative and quantitative information is presented and the analytical potential of the proposed method is discussed. Finally, the specific application of the proposed method to wine analysis is demonstrated and the method is compared with the standard reference methods for wine analysis [31]. These reference methods are single component determinations and they are based mainly on time-consuming enzymatic methods (fructose, glucose, glycerol, citric acid, malic acid and lactic acid). Exceptions are ethanol and tartaric acid, which are determined by distillation and gravimetrically after precipitation.

## 2. Experimental

### 2.1. Reagents

Standard solutions were prepared by dissolving an appropriate amount of each analyte in distilled water. All substances were either of analytical grade or for biochemical use (>99%) from standard suppliers (Merck, Darmstadt, Germany; Sigma, St. Louis, MO, USA; Aldrich, Milwaukee, WI, USA); L(+)-lactic acid (>99%) was obtained from Fluka (Buchs, Switzerland). Standard solutions were stabilized with 50 mg/l  $\text{NaN}_3$  and stored for 48 h before use in order to prevent mutarotational effects on the glucose and fructose spectra [30]. The wine samples (three white and three red wines) were provided by the Institute for Beverage Analysis (Bundesamt und Forschungszentrum für Landwirtschaft, Vienna, Austria). The reference data were obtained according to the official Austrian analysis methods for wine

analysis [31] and they were verified by a round robin test. For the HPLC–FTIR analysis, the wine samples were filtered (0.45  $\mu\text{m}$ ) prior to injection, this being the only preparation step.

## 2.2. HPLC

The HPLC system consisted of a Merck/Hitachi L7100 isocratic pump (flow-rate, 0.5 ml/min) and a Rheodyne 7725 injection valve (injection volume: 20 or 50  $\mu\text{l}$ ). The mobile phase was 0.005 M  $\text{H}_2\text{SO}_4$ , which ensured that all organic acids were undissociated. Degassing of the mobile phase prior to use was found not to be necessary for maintaining a constant flow-rate.

Furthermore, an in-line filter and a 30 $\times$ 4.6 mm guard column were employed to protect the 250 $\times$ 7.8 mm analytical column (Inores H, purchased from Inovex, Vienna, Austria). The stationary phase of both the analytical and guard columns was a polystyrene divinylbenzene anionic-exchange resin with  $\text{H}^+$  counter-ion (particle size, 8  $\mu\text{m}$ ; crosslinkage, 8%). Instead of a column oven, a modified glass tube connected with a thermostated water bath was used for temperature control of the column. All connections were made of polyetheretherketone (PEEK) tubing with an I.D.s of 0.25 and 0.17 mm.

## 2.3. IR flow cell

A standard Perkin-Elmer transmission flow cell with an optical pathlength of 25  $\mu\text{m}$  and  $\text{CaF}_2$  windows (of 2 mm thickness each) was used, yielding an approximately  $1/e$  attenuation (absorbance  $\sim 0.4$ ) of the water background absorption at 1100  $\text{cm}^{-1}$ . The volume of the cell used was 10  $\mu\text{l}$ . Special care was taken to reduce the void volume between the flow cell and the PEEK tubing to prevent peak broadening. The  $\text{CaF}_2$  windows were coated with a protective layer of low density polyethylene (LDPE), since  $\text{CaF}_2$  windows are slightly soluble in acidic solutions such as the sulfuric acid-containing mobile phase used in this work. This was done simply by dip-coating the  $\text{CaF}_2$  windows in a 2% solution of LDPE (low molecular mass) in decahydronaphthalene at 120°C. The thickness of the coating was found to be in the range of 1  $\mu\text{m}$ . The

LDPE coating was stable for at least 48 h. Protective inorganic coatings, such as silicon oxide and silicon nitride (physical vapor deposition) and carbon (laser ablation deposition), were also investigated, but the unavoidable tensions of the flow cell induced cracking and a rapid detachment of these layers. The relatively poor long-term stability of the polymer coating used here might present a drawback for industrial applications. However, it is supposed that further improvements of window materials or coating techniques (e.g. diamond-like carbon) will make this analytical technique applicable for an industrial environment.

## 2.4. FTIR parameters

Infrared measurements were performed on a Bruker IFS 88 FTIR spectrometer equipped with a liquid nitrogen-cooled narrow band MCT detector ( $D^* = 2.10^{10} \text{ cm Hz}^{1/2} \text{ W}^{-1}$ ). As presented in previous work by our group [32–34], a significant increase in the signal-to-noise ratio of FTIR measurements in the spectral region of interest (1600–900  $\text{cm}^{-1}$ ) is achievable by the introduction of a low wave pass filter (5% cut off, 1700  $\text{cm}^{-1}$ ) into the optical setup. By means of this filter, the radiation intensity in the region of interest can easily be increased by opening the aperture without causing oversaturation of the highly sensitive narrow band MCT detector. Hence, an improved limit of detection is achieved, which is accompanied by a reduction in qualitative information (reduction of the multiplex advantage), because the spectral range above 1700  $\text{cm}^{-1}$  is no longer accessible when using the optical filter. However, for the analysis of carbohydrate absorption patterns and for the general investigation of CO bondings, the range from 900–1600  $\text{cm}^{-1}$  is the region of interest. For the analysis of (undissociated) organic acids, the C=O vibration at 1700–1740  $\text{cm}^{-1}$  is also of principal interest. However, these bands are too close to the strong water band at 1640  $\text{cm}^{-1}$  (O–H bending) to provide valuable quantitative information.

## 2.5. Data acquisition and evaluation

For each spectrum recorded during a HPLC–FTIR run, 50 scans were coadded. The resolution of all

spectra was  $8\text{ cm}^{-1}$ , the scanner velocity was set to 80 kHz (HeNe frequency). The total acquisition time including Fourier-transformation and further data processing was approximately 3.1 s, resulting in sufficient time resolution of 19 spectra per minute.

Standard Bruker GC–LC software was used for convenient 3D data treatment and postrun trace calculation. Selective HPLC traces were calculated from the 3D recording with respect to the absorption of the analytes by choosing the appropriate peak and baseline wavenumbers. Interferogram domain data evaluation, such as Gram Schmidt traces, could not be used successfully, which is explained by the strong background absorption of water. It is assumed that slight drifts in the matrix background absorption cause a greater change in the interferograms than the small changes due to analyte absorption. The integration of the chromatographic peaks was done using the software provided by the spectrometer manufacturer.

### 3. Results and discussion

#### 3.1. HPLC–FTIR chromatograms

A typical three-dimensional HPLC–FTIR chromatogram is given in Fig. 1. For that chromatogram, 50  $\mu\text{l}$  of a standard solution containing 2 mg/ml of each analyte was injected. The advantage of multi-dimensional detection in the mid infrared region

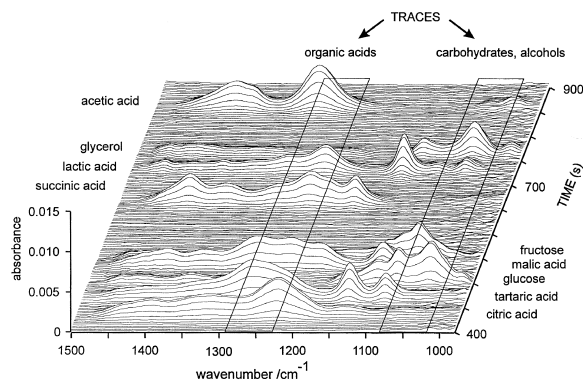


Fig. 1. Typical HPLC–FTIR run of a standard solution containing 2 mg/ml of the main components of wine. Only retention times from 400 to 900 s are presented for better visualization (injection volume, 50  $\mu\text{l}$ ; column temperature, 70°C).

(MIR) is obvious. Each compound eluted gave a distinct spectrum, providing good qualitative information for its identification. The traces following the change in absorption at the appropriate wavenumbers can be drawn along the time axis. The spectral region of two traces, one selective for carbohydrates and alcohols ( $1050\text{ cm}^{-1}$ ), and another for organic acids ( $1260\text{ cm}^{-1}$ ), are visualized in Fig. 1. The corresponding traces are depicted in Fig. 2. In order to minimize drift effects in the baseline of the FTIR spectra, baseline points were chosen close to the characteristic absorption bands of carbohydrates and organic acids to calculate the corresponding traces. This is also the reason for the slightly negative peaks present in Fig. 2. The solvent peak at 4.7 min displays the decrease in sulfate absorption (maximum at  $1105\text{ cm}^{-1}$ ) due to sample injection (compared to the 0.005 M  $\text{H}_2\text{SO}_4$  of the eluent). Glucose (3) malic acid (4) and fructose (5) are not completely baseline separated but by focusing on the two selective traces, an apparent separation is achieved and the quantitative evaluation is not biased by the incomplete chromatographic separation.

#### 3.2. Temperature dependency of the elution

The interactions in ion-exchange chromatography are intensely dependent on the column temperature.

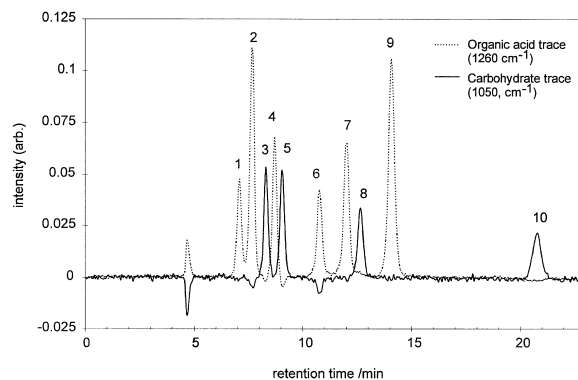


Fig. 2. Two HPLC–FTIR traces extracted from Fig. 1. One trace (dotted line) represents the absorption at  $1260\text{ cm}^{-1}$  and is sensitive to the organic acids. In the second trace (solid line), the absorptions at  $1050\text{ cm}^{-1}$  are extracted to visualize the carbohydrates and alcohols. Peak identification: 1, citric acid; 2, tartaric acid; 3, glucose; 4, malic acid; 5, fructose; 6, succinic acid; 7, lactic acid; 8, glycerol; 9, acetic acid and 10, ethanol.

For studying retention times as a function of column temperature, the FTIR detector serves as a convenient tool for the immediate identification of the compounds. The traces of a HPLC–FTIR chromatogram at three different temperatures are presented in Fig. 3. By focussing on the two traces for organic acids ( $1260\text{ cm}^{-1}$ ) and for carbohydrates ( $1050\text{ cm}^{-1}$ ), the elution behavior can be observed directly. Whereas the retention times of the sugars and alcohols are not seriously effected by the column temperature, the organic acids elute significantly earlier at higher temperatures. As a result, a change in the elution order of tartaric acid (2) and glucose (3), as well as the sequence of malic acid (4) and fructose (5) is noticed. By means of HPLC–FTIR, it

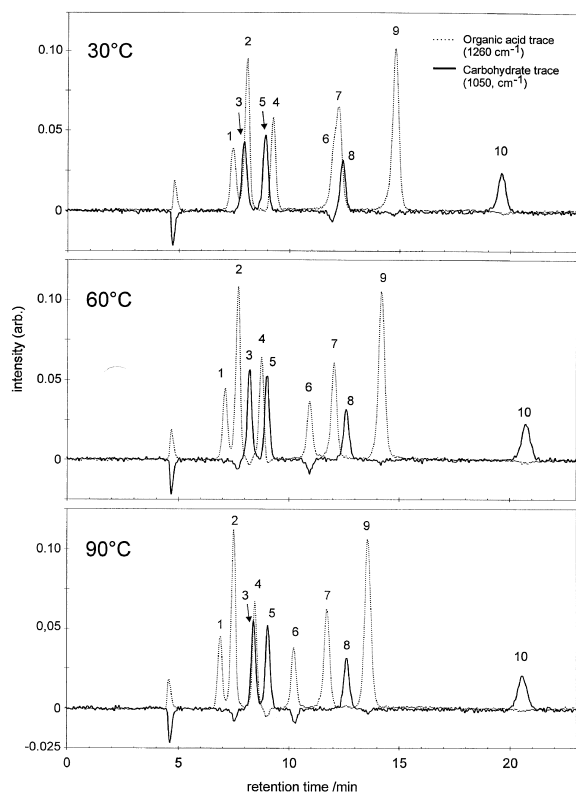


Fig. 3. HPLC–FTIR traces of a standard solution containing 2 mg/ml of each compound (injection volume, 50  $\mu\text{l}$ ). Variation of the column temperature caused a change in the elution sequence [see malic acid (4) and fructose (5)]. This is easily recognized by the molecular specific FTIR detection. Also, the detection of two overlapping substance peaks is feasible (for peak identification, see Fig. 2).

is also possible to determine quantitatively overlapping peaks [see glucose (3) and malic acid (4) at  $90^\circ\text{C}$ ]. An identification of the compounds is possible on the basis of compound-characteristic spectral features, which are not overlapping in the mixed IR spectra.

### 3.3. Extraction of the FTIR spectra

The spectra of all investigated compounds were extracted from the 3-D data set and are displayed in Fig. 4. The high quality of these spectra allows us to use them for identification purposes. In the experi-

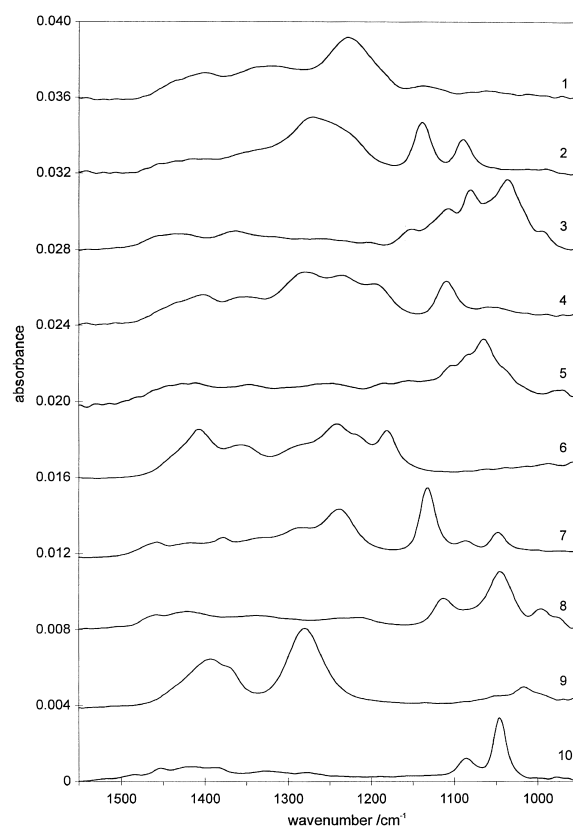


Fig. 4. Identifiable spectra extracted from a HPLC–FTIR run of a standard solution containing 2 mg/ml of each compound (injection volume, 50  $\mu\text{l}$ ). Note that acid spectra are in the protonated state at pH 2 and glucose and fructose spectra are recorded in anomeric equilibrium. Spectra: 1, citric acid; 2, tartaric acid; 3, glucose; 4, malic acid; 5, fructose; 6, succinic acid; 7, lactic acid; 8, glycerol; 9, acetic acid and 10, ethanol (offset of 0.004 for each spectrum).

ment, 50  $\mu\text{l}$  of a 2 mg/ml solution of each compound were injected. In order to reduce the spectral noise, several spectra were averaged over the chromatographic peak maximum. For the identification of these spectra and comparison with library data, two points have to be taken into consideration. The glucose and fructose spectra are recorded from the equilibrium of both  $\alpha$ - and  $\beta$ -anomers at that temperature and pH. As an example, both  $\alpha$ - and  $\beta$ -glucose exhibit complete different absorption spectra in the mid-IR range [30]. Secondly, the organic acids that were investigated in this study are present in the protonated state at pH 2 and show a completely different spectrum compared to that obtained when they are in their dissociated states.

Nevertheless, spectra of reasonable  $S/N$  were achieved, allowing for the unambiguous identification of the analytes by focussing on both the characteristic retention times and the mid-IR spectra of the analytes. From these spectra, the identification limit can be estimated to be less than 1 mg/ml, resulting in an absolute identification limit of 50  $\mu\text{g}$ .

### 3.4. Calibration with standard solutions

The performance of the proposed system was

studied by calibrating with standard solutions. The injection volume was reduced to 20  $\mu\text{l}$  for the calibration as well as for the analysis of real wine samples. The concentration range chosen was 1, 2.5, 5, 7.5 and 10 mg/ml for all analytes except ethanol. For the analysis of wines, a tenfold ethanol concentration was used. Five standards were prepared, containing each of the ten compounds at different concentrations. In this way, the calibration system was also sensitive to cross-interferences, e.g. of co-eluting substances. The calibration parameters and results are listed in Table 1. The precision was further optimized by extracting the optimal traces for each analyte. The peak wavenumbers and baseline points were chosen for each compound according to their IR spectra (Fig. 4). For analytes exhibiting two (lactic acid, acetic acid) or three (tartaric acids) absorption bands, two or three traces were extracted from the HPLC–FTIR chromatograms and summed up. For each analyte, a linear five-point calibration graph was obtained. The precision was evaluated by the standard deviation of the method  $s_{x0}$ , calculated as the ratio of the residual standard deviation,  $s_y$ , and the slope (according to ISO 8466-1). The average standard deviation found was 66  $\mu\text{g/ml}$ . The limit of detection (LOD), estimated as the threefold standard

Table 1  
Calibration data and results

Analyte	Calibration range (mg/ml)	Peak(s) for trace calculation <sup>a</sup> ( $\text{cm}^{-1}$ )	Retention time (min)	Standard deviation <sup>b</sup> (mg/ml)	$R^2$
Ethanol	10–100	1045 (1021, 1066)	20.8	0.11	0.999992
Glycerol	1–10	1044 (1008, 1084) 1115 (1158, 1085)	12.7	0.024	0.999996
Glucose	1–10	1035 (1000, 1058)	8.3	0.080	0.999951
Fructose	1–10	1065 (1007, 1148)	9.0	0.016	0.999998
Acetic acid	1–10	1280 (1200, 1335) 1395 (1335, 1475)	14.1	0.066	0.999967
Citric acid	1–10	1228 (1158, 1283)	7.1	0.109	0.999911
Lactic acid	1–10	1132 (1100, 1170)	12.0	0.046	0.999984
Malic acid	1–10	1111 (1056, 1146) 1200 (1141, 1512)	8.7	0.051	0.999981
Succinic acid	1–10	1242 (1120, 1322)	10.8	0.082	0.999949
Tartaric acid	1–10	1090 (1050, 1111) 1139 (1111, 1175) 1268 (1175, 1333)	7.7	0.071	0.999963

<sup>a</sup> Baseline points are in brackets.

<sup>b</sup> Standard deviation of the method according to ISO 8466-1 (1990).

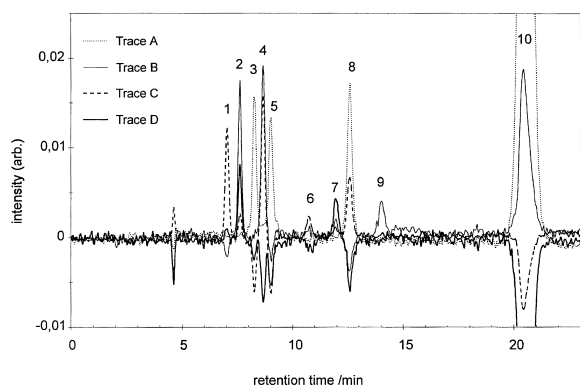


Fig. 5. HPLC–FTIR run of a wine sample (injection volume, 20  $\mu$ l; column temperature, 70°C). Four traces were extracted. Trace A (1050  $\text{cm}^{-1}$ ) shows the maximum sensitivity for glucose (3), fructose (5), glycerol (8) and ethanol (10). Trace B (1280, 1395  $\text{cm}^{-1}$ ) shows the maximum sensitivity for tartaric acid (2), malic acid (4) and acetic acid (9). Trace C (1228  $\text{cm}^{-1}$ ) shows the maximum sensitivity for citric (1) and succinic acid (6). Trace D (1132  $\text{cm}^{-1}$ ) shows the maximum sensitivity for lactic acid (7).

deviation, was 0.2 mg/ml. The corresponding absolute LOD was therefore 4  $\mu$ g (20  $\mu$ l injection volume). It is interesting to note that the standard deviation of the tenfold higher ethanol concentration is not significantly higher, but remains in the range of 110  $\mu$ g/ml. Ethanol has the longest retention time (20.8 min) and is well isolated from the next substance (acetic acid, 14.1 min). Therefore, it can be concluded that, insofar as peak broadening does not lead to strong overlapping, the precision is negligibly

effected by the concentrations injected. Hence, an increase of the injection volume should lead to enhanced precision. However, the influence of large injection volumes of real samples on column aging has to be taken into consideration.

### 3.5. Wine sample determination

In a final step, the proposed method was applied to wine samples as a real matrix. The separation of a wine sample is shown in Fig. 5. Since some compounds are present at concentrations less than 1 mg/ml, four traces have been extracted for visualizing all ten of the analytes investigated. The corresponding concentrations of that sample (wine sample A) are listed in Table 2. Acetic acid (0.15 mg/ml) and lactic acid (0.41 mg/ml) exhibit significant peaks in the HPLC–FTIR traces.

The HPLC–FTIR results and the reference data are listed in Table 2. However, for acetic and succinic acid, no reference values were available, because neither belongs to the standard control parameters for wines. The deviations found were less than 1 mg/ml in all cases. The average deviation of 0.16 mg/ml is in a similar range as the deviations obtained from the standard solutions (0.066 mg/ml), which demonstrates the performance of the proposed system.

The detection limits obtained using commercially available enzymatic methods, as used for these compounds, is about two orders of magnitude lower.

Table 2  
HPLC–FTIR results of Austrian real wine samples

	A	B	C	D	E	F
Ethanol	79.56 (79.5)	94.11 (93.9)	85.43 (84.5)	89.33 (89.1)	91.51 (92.2)	96.00 (95.5)
Glycerol	5.93 (5.8)	8.10 (8.0)	7.36 (7.2)	7.49 (7.5)	7.13 (7.0)	8.76 (8.8)
Glucose	2.65 (2.8)	0.35 (0.4)	5.69 (6.4)	6.94 (7.7)	3.71 (3.9)	0.15 <sup>a</sup> (0.2)
Fructose	3.57 (3.5)	1.48 (1.4)	7.29 (7.3)	7.49 (7.6)	3.71 (3.8)	0.06 <sup>a</sup> (0.1)
Acetic acid	0.15 <sup>a</sup>	0.25	0.21	0.57	0.53	0.65
Citric acid	1.17 (1.2)	0.29 (0.3)	1.00 (1.0)	1.56 (1.7)	0.89 (0.9)	0.16 <sup>a</sup> (0.2)
Lactic acid	0.41 (0.3)	0.56 (0.4)	0.44 (0.4)	2.80 (2.6)	2.66 (2.5)	3.37 (3.1)
Malic acid	2.37 (2.4)	3.17 (3.3)	2.87 (3.0)	−0.03 <sup>a</sup> (0.0)	0.02 <sup>a</sup> (0.0)	0.00 <sup>a</sup> (0.0)
Succinic acid	0.40	0.55	0.50	0.48	0.45	0.58
Tartaric acid	1.19 (0.9)	1.68 (1.2)	1.57 (1.1)	1.14 (0.9)	1.06 (0.8)	1.31 (1.0)

Reference data in brackets were validated by a round robin test.

All concentrations are given in mg/ml (A–C, white wine and D–F, red wine).

<sup>a</sup> Value was below the detection limit.

The comparatively low sensitivity of aqueous phase HPLC–FTIR is compensated for by the high speed of multi-component analysis, the low cost per analysis and the high degree of automation.

#### 4. Conclusion

This work shows the potential of this advanced flow cell-based HPLC–FTIR setup for aqueous eluents, which has not only been shown for standard solutions, but also for complex real matrices such as wines. The capability of real time HPLC–FTIR for the determination of carbohydrates, alcohols and organic acids in wines was demonstrated for the first time. Whereas organic acids are also easily detected by UV spectroscopic methods, the molecular specific FTIR detection is a very promising alternative for carbohydrates and alcohols. The detection limit of 0.2 mg/ml for these compounds demonstrates that the common opinion in the literature, stating that flow cell-based FTIR detection is incompatible or too insensitive [2–4] for practical applications in aqueous phase HPLC, will have to be seen in a new and modified way.

Although FTIR detection provides the possibility of identifying substance classes that cannot be determined by UV–Vis methods, it has to be stated that the conventional (KBr) IR spectra libraries generally cannot be applied for the identification of substances in aqueous solution.

Further improvements of real time HPLC–FTIR will be made not only by experimental and spectroscopic progress but also by the application of multivariate data-processing techniques. It is expected that automatic compound identification and an additional gain in precision are feasible with chemometric methods.

#### Acknowledgements

The authors want to thank Dr. Bandion, Institut für Getränkeanalytik, Bundesamt und Forschungszentrum für Landwirtschaft in Austria for providing the wine samples and the round robin test data. Financial support of this work from the ‘Fonds zur Förderung

der wissenschaftlichen Forschung, P11338ÖCH’ is gratefully acknowledged.

#### References

- [1] C. Fujimoto, K. Jinno, *Trends Anal. Chem.* 8 (1989) 90.
- [2] R. White, *Chromatography/Fourier Transform Infrared Spectroscopy and Its Applications*, Marcel Dekker, New York, 1990.
- [3] K. Jinno, in E.S. Yeung (Editor), *Detectors for Liquid Chromatography*, Chemical Analysis 89, Wiley, New York, 1986, Ch. 3, p. 78.
- [4] V.F. Kalasinsky, K.S. Kalasinsky, in G. Patonay (Editor), *HPLC Detection, Newer Methods*, VCH, New York, 1992, Ch. 7, p. 127.
- [5] J.J. Gagel, K. Biemann, *Anal. Chem.* 59 (1987) 1266.
- [6] J. Yang, P.R. Griffiths, *Proc. SPIE* 2089 (1993) 336.
- [7] A.J. Lange, P.R. Griffiths, *Appl. Spectrosc.* 47 (1993) 403.
- [8] A.J. Lange, P.R. Griffiths, D.J.J. Fraser, *Anal. Chem.* 63 (1991) 782.
- [9] M.A. Castles, L.V. Azarraga, L.A. Carreira, *Appl. Spectrosc.* 40 (1986) 673.
- [10] M.W. Raynor, K.D. Bartle, B.W. Cook, *J. High Resolut. Chromatogr.* 15 (1992) 361.
- [11] R.M. Robertson, J.A. de Haseth, J.D. Kirk, R.F. Browner, *Appl. Spectrosc.* 42 (1988) 1365.
- [12] R.M. Robertson, J.A. de Haseth, R.F. Browner, *Appl. Spectrosc.* 44 (1990) 8.
- [13] V.E. Turula, J.A. de Haseth, *Anal. Chem.* 68 (1996) 629.
- [14] V.E. Turula, J.A. de Haseth, *Appl. Spectrosc.* 48 (1994) 1255.
- [15] A.M. Robertson, L. Wylie, D. Littlejohn, R.J. Watling, C.J. Dowle, *Anal. Proc.* 28 (1991) 8.
- [16] A.M. Robertson, D. Littlejohn, M. Brown, C.J. Dowle, *J. Chromatogr.* 588 (1991) 15.
- [17] A.M. Robertson, D. Farnan, D. Littlejohn, M. Brown, C.J. Dowle, E. Goodwin, *Anal. Proc.* 30 (1993) 268.
- [18] C.C. Johnson, J.W. Hellgeth, L.T. Taylor, *Anal. Chem.* 57 (1985) 610.
- [19] J.W. Hellgeth, L.T. Taylor, *Anal. Chem.* 59 (1987) 295.
- [20] C.M. Conroy, P.R. Griffiths, P.J. Duff, L.V. Azarraga, *Anal. Chem.* 56 (1984) 2636.
- [21] G.W. Somsen, E.W.J. Hooijschuur, C. Gooijer, U.A.Th. Brinkman, N.H. Velthorst, T. Visser, *Anal. Chem.* 68 (1996) 746.
- [22] M. Sabo, J. Gross, J. Wang, I.E. Rosenberg, *Anal. Chem.* 57 (1985) 1822.
- [23] A. Rein, P. Wilks, *Am. Lab.* 14(10) (1982) 152.
- [24] P.T. McKittrick, N.D. Danielson, J.E. Katon, *J. Liq. Chromatogr.* 14(2) (1991) 377.
- [25] C. Fujimoto, K. Jinno, *Trends Anal. Chem.* 8 (1989) 90.
- [26] K. Jinno, C. Fujimoto, *J. Chromatogr.* 506 (1990) 443.
- [27] C. Fujimoto, G. Uematsu, K. Jinno, *Chromatographia* 20 (1985) 112.



- [28] A. Tartar, J.P. Huvenne, H. Gras, C. Sergheraert, *J. Chromatogr.* 298 (1984) 521.
- [29] R. Vonach, B. Lendl, R. Kellner, *Anal. Chem.* 69 (1997) 4286.
- [30] D.M. Black, D.F. Michalska, P.L. Polavaparu, *Appl. Spectrosc.* 38 (1984) 173.
- [31] Austrian Federal Law, Methodenverordnung BGBl 495/1989.
- [32] P. Krieg, B. Lendl, R. Vonach, R. Kellner, *Fresenius' J. Anal. Chem.* 356 (1996) 504.
- [33] R. Vonach, R. Kellner, M. Lippitsch, *Proceedings of EURO FOOD CHEM VIII*, Vienna, 1995, p. 573.
- [34] R. Vonach, B. Lendl, R. Kellner, *Analyst* 122 (1997) 525.